

This is an Open Access document downloaded from ORCA, Cardiff University's institutional repository: <https://orca.cardiff.ac.uk/id/eprint/167328/>

This is the author's version of a work that was submitted to / accepted for publication.

Citation for final published version:

Zheng, Lianming, Adalibieke, Wulahati, Zhou, Feng, He, Pan , Chen, Yilin, Guo, Peng, He, Jinling, Zhang, Yuanzheng, Xu, Peng, Wang, Chen, Ye, Jianhuai, Zhu, Lei, Shen, Guofeng, Fu, Tzung-May, Yang, Xin, Zhao, Shunliu, Hakami, Amir, Russell, Armistead G., Tao, Shu, Meng, Jing and Shen, Huizhong 2024. Health burden from food systems is highly unequal across income groups. *Nature Food* 5 , pp. 251-261.
10.1038/s43016-024-00946-7

Publishers page: <http://dx.doi.org/10.1038/s43016-024-00946-7>

Please note:

Changes made as a result of publishing processes such as copy-editing, formatting and page numbers may not be reflected in this version. For the definitive version of this publication, please refer to the published source. You are advised to consult the publisher's version if you wish to cite this paper.

This version is being made available in accordance with publisher policies. See <http://orca.cf.ac.uk/policies.html> for usage policies. Copyright and moral rights for publications made available in ORCA are retained by the copyright holders.



1 **Health burden from food systems is highly unequal across**
2 **income groups**

3 Lianming Zheng^{1,2}, Wulahati Adalibieke³, Feng Zhou^{3,4,*}, Pan He^{5,*}, Yilin Chen^{1,2,6}, Peng Guo^{1,2},
4 Jinling He^{1,2}, Yuanzheng Zhang³, Peng Xu⁷, Chen Wang^{1,2}, Jianhuai Ye^{1,2}, Lei Zhu^{1,2}, Guofeng Shen³,
5 Tzung-May Fu^{1,2}, Xin Yang^{1,2}, Shunliu Zhao⁸, Amir Hakami⁸, Armistead G. Russell⁹, Shu Tao^{1,2,3}, Jing
6 Meng^{10,*}, Huizhong Shen^{1,2,*}

7 ¹Shenzhen Key Laboratory of Precision Measurement and Early Warning Technology for Urban
8 Environmental Health Risks, School of Environmental Science and Engineering, Southern University
9 of Science and Technology, Shenzhen, Guangdong, China

10 ²Guangdong Provincial Observation and Research Station for Coastal Atmosphere and Climate of
11 the Greater Bay Area, Southern University of Science and Technology, Shenzhen, Guangdong, China

12 ³Institute of Carbon Neutrality, Laboratory for Earth Surface Processes, College of Urban and
13 Environmental Sciences, Peking University, Beijing, China

14 ⁴College of Geography and Remote Sensing, Hohai University, Nanjing, Jiangsu, China

15 ⁵School of Earth and Environmental Sciences, Cardiff University, Cardiff, Wales, United Kingdom

16 ⁶School of Urban Planning and Design, Peking University, Shenzhen Graduate School, Shenzhen,
17 Guangdong, China

18 ⁷Institute of Surface-Earth System Science, School of Earth System Science, Tianjin University,
19 Tianjin, China

20 ⁸Department of Civil and Environmental Engineering, Carleton University, Ottawa, ON, Canada

21 ⁹School of Civil and Environmental Engineering, Georgia Institute of Technology, Atlanta, Georgia,
22 United States

23 ¹⁰The Bartlett School of Sustainable Construction, University College London, London, United
24 Kingdom

25 *Corresponding author, e-mail: zhoulf@pku.edu.cn; hep3@cardiff.ac.uk; jing.j.meng@ucl.ac.uk;
26 shenhz@sustech.edu.cn

27

28 **Abstract**

29 Food consumption contributes to the degradation of air quality in regions where food is produced,
30 creating a contrast between the health burden caused by a specific population through its food
31 consumption and that faced by this same population as a consequence of food production
32 activities. Herein, we explore this inequality within China's food system by linking air pollution-
33 related health burden from production to consumption, at high levels of spatial and sectorial
34 granularity. We find that low-income groups bear a 70% higher air pollution-related health burden
35 from the food production than is caused by their food consumption, while high-income groups
36 benefit from a 29% lower health burden relative to their food consumption. This discrepancy
37 largely stems from a concentration of low-income residents in food production areas, exposed to
38 higher emissions from agriculture. Comprehensive interventions targeting both production and
39 consumption sides can effectively reduce health damages and concurrently mitigate associated
40 inequalities, while singular interventions exhibit limited efficacy.

41 **Introduction**

42 Agricultural intensification and redistribution have significantly increased food productivity and the
43 abundant and diverse food supply^{1,2}. However, these practices have also resulted in an uneven
44 distribution of the environmental footprint of the food system. Emissions embedded in the food
45 system are spread across various food-producing regions that may be far from where the food is
46 consumed. Globally, 26%–64% of the population cannot fulfill their crop demand solely through
47 crop production within a 1000-km radius³. In China, Henan, Hebei, and Shandong provinces
48 accounted for about one-third of agricultural ammonia (NH₃) emissions⁴, while local food
49 consumption only constituted 11%–19% of the national food consumption⁵. Consequently, food
50 contributes one of the greatest disparities in consumption-based PM_{2.5} (fine particulate matter
51 with diameter <2.5 μm) pollution exposure among all goods⁶, potentially leading to significant
52 environmental inequality among different groups of people. In the United States, non-Hispanic
53 whites exhibit higher food consumption rates and consequently cause a 61% greater air pollution
54 exposure compared to their black and Hispanic counterparts⁶.

55 In alignment with the United Nations Sustainable Development Goals, the modern food system
56 needs to feed the global population to provide nutritional security with low environmental impact
57 and without contributing to social injustice⁷⁻¹³. To avoid a disproportionate allocation of health

58 outcomes to a small subset of the population, a key step is to explicitly evaluate the inequality of
59 the health damage attributed to the food system, which is rarely discussed. Key factors such as
60 food categories, spatial heterogeneity, and potential drivers (e.g., household wealth) have not
61 been adequately explored, impeding efforts to reduce inequality. Taking food categories as an
62 example, ruminant meat, especially beef, has the highest environmental impact compared to non-
63 ruminant meat, whereas plant-based foods have the least impact^{14,15}. However, the manner and
64 degree to which food categories affect general health-related inequalities remain unknown, and it
65 is unclear whether existing intervention strategies aimed at alleviating environmental burdens and
66 mitigating the negative health effects of the food system can provide co-benefits in reducing
67 related inequalities.

68 Expanding on this concept, we examine the air pollution–related inequality within China’s food
69 system. As the world’s leading agricultural producer, China has experienced significant agricultural
70 intensification¹⁶. This transformation is partially driven by the nutritional requirements of its
71 sizable population, exacerbated by the limited per-capita arable land compared to the global
72 average¹⁷. The inherent contradiction arising from the restricted agricultural land and the
73 escalating food demand has necessitated farmers to enhance their food production efficiency,
74 thereby fueling the process of agricultural intensification. These factors and a diverse dietary
75 transition¹⁸ make China’s food system an important case for understanding air pollution–related
76 inequality.

77 **Results**

78 **Spatial heterogeneity in air pollution–related health impact**

79 We quantified air pollution–related health damage, represented by premature mortality,
80 throughout the food supply chain. Our analytical framework integrates several components: a
81 high-resolution emission inventory with 1 km × 1 km resolution for NH₃ emissions from cropland
82 and livestock management, developed by Adalibieke et al.¹⁹ and Wang et al.²⁰ as well as 10 km ×
83 10 km resolution for NH₃ emissions from non-agricultural activities²¹ and other pollutants (e.g.,
84 primary PM_{2.5}, SO₂, NO_x) from all sources²²⁻²⁵, derived from the PKU Inventory for the baseline year
85 2017 (see Methods and Data); a provincial-level input–output table; and an advanced backward
86 sensitivity analysis technique implemented within a regional chemical transport model (CMAQ-
87 Adjoint)²⁶. Using the adjoint model enabled us to trace air pollution–related health damage from

88 production to consumption across nine distinct food categories at a high level of spatial and
89 sectoral granularity (Methods and Data). This fine resolution facilitated the investigation of air
90 pollution–related inequality within the food system.

91 In general, the food system in China was responsible for approximately 0.26 (95% confidence
92 interval (CI), [0.22, 0.32]) million premature deaths related to ambient PM_{2.5} exposure in 2017.
93 Most (74%) of these deaths are attributed to NH₃ emissions, an important precursor of ambient
94 PM_{2.5}, during food production, such as crop cultivation and livestock breeding. The remainder (26%)
95 are caused by emissions of primary PM and other precursors, including SO₂ from power plants and
96 NO_x from motor vehicles, during the distribution, aggregation, processing, packaging, and
97 marketing of food products. This food–induced air pollution-related mortality represents 12% of
98 overall annual mortality from exposure to ambient PM_{2.5} in China. Of this mortality, meat
99 contributes 55%; grains contribute 30%; and vegetables, fruits, and non-meat animal products
100 (including eggs and dairy) account for the remaining 15% (see Supplementary Text1 for a
101 comparative analysis of our results and previous studies).

102 Northern and Eastern China are the regions most affected by food production (Fig. 1a and
103 Supplementary Fig. 1a), and 41% of the mortality is attributable to food production (defined as
104 “ M_p ”) concentrated in Shandong, Henan, Hebei, and Jiangsu (Supplementary Fig. 1a). The spatial
105 distribution is determined by regional population levels (Supplementary Fig. 2a) and agricultural
106 NH₃ emissions (Supplementary Fig. 2b) in conjunction. The Gini coefficient, representing the
107 inequality of spatial disparity for M_p , is estimated to be 0.31 on average and ranges from 0.30 to
108 0.64 by food type (Fig. 1d and Supplementary Fig. 3). The Gini coefficient of overall food in
109 mortalities is relatively low compared to that of specific food types. This can be attributed to the
110 evident spatial variation in the distribution of mortality rates caused by different food types
111 (Supplementary Fig. 4), thereby mitigating the disparities in the spatial distribution of cumulative
112 mortality rates.

113 The distribution of premature mortality rates based on food consumption (“ M_c ” rates) is more
114 dispersed than that of M_p rates (Fig. 1b). The provinces with the highest air pollution–related
115 mortality rates from their food consumption are Shanxi, Inner Mongolia, Shandong, Hubei, and
116 Jiangsu. Two categories of regions emerged. The first category pertains to highly developed regions
117 with wealthy populations, such as Beijing, Shanghai, Zhejiang, and Guangdong, which show higher

118 M_C rates than the others. The second category represents concentrated food-producing regions
119 with developed agricultural production, such as Henan and Hebei, where M_C is far below M_P . The
120 distribution of M_C is more closely associated with the spatial differences in population and regional
121 dietary preferences, particularly in grains and meats consumption (Supplementary Fig. 5). The
122 spatial inequality of M_C is significantly lower than that of M_P , with a Gini coefficient of 0.21 on
123 average (ranging from 0.23 to 0.53 across different food types; Fig. 1d and Supplementary Fig. 3).
124 Similar to M_P , the Gini coefficient of total mortality is lower, since the spatial heterogeneity of
125 mortalities of different food type (Supplementary Fig. 6). The low inequality of M_C is attributed to
126 a convergence toward a modernized diet (Supplementary Fig. 7) characterized by high meat
127 consumption in the last few decades⁵, which is consistent with global patterns^{27,28}.

128 **Inequality by food categories**

129 We calculated the difference between M_P and M_C rates, presented as ΔM rate in Fig. 1c (Methods
130 and Data). Positive ΔM rates indicate that people in the region face a larger health burden from
131 food production than that caused by food consumption (“production-oriented”), whereas negative
132 ΔM rates signify the opposite (“consumption-oriented”). Overall, the ΔM rates vary geographically
133 across the country. The consumption-oriented provinces include (1) regions with poor crop-
134 growing conditions (e.g., Qinghai and Tibet) that face constraints with regard to food production
135 and (2) highly developed regions (including provincial-level municipalities, such as Chongqing and
136 Beijing, and coastal provinces, such as Zhejiang) where the industrial focus has shifted from
137 agriculture to other industries²⁹. Notably, the results of ΔM rates are strongly influenced by
138 population size, as the considerable difference between the M_P and M_C rates in the total mortality
139 would be scaled down owing to the high population in per-capita terms (e.g., Guangdong, as shown
140 in Supplementary Fig. 1a, b) and vice versa (e.g., Tibet, Hainan, and Qinghai; Supplementary Fig.
141 1a, b).

142 Henan exhibited the highest positive ΔM rate, with 1.06 (95% CI: [0.00, 2.13]) premature deaths
143 per 10,000 population. This region experiences severe food-induced air pollution, which locally
144 causes 2.95 (95% CI: [0.93, 4.97]) premature deaths per 10,000 population. Comparatively, food
145 consumption in Henan is responsible for 1.88 (95% CI: [0.91, 2.86]) premature deaths per 10,000
146 population nationwide. Thus, the population in Henan bears a 57% higher health burden due to
147 food production than that caused by their food consumption. Conversely, Beijing exhibited the

148 lowest ΔM rate, with a value of -1.32 (95% CI, $[-0.88, -1.77]$; 0.74 (95% CI, $[0.24, 1.25]$) and 2.06
149 (95% CI, $[1.59, 2.55]$) for the M_p and M_c rates, respectively, and a 64% lower health burden). Given
150 the limitations of existing inequality metrics, such as the Gini coefficient and the pollution inequity
151 index proposed by Tessum et al.⁶, in evaluating the inequality between production and
152 consumption (i.e., ΔM rates with both positive and negative values), we developed a Supply–
153 Demand Health Inequality Index (SDHII) to estimate national inequality in the ΔM rates. This index
154 incorporates the discrepancy between the production- and consumption-based mortality rates of
155 individual population groups and weights them by population size to get the final national-level
156 inequality. As a result, this index evaluates the inequality compared with an ideal state of complete
157 equality (Methods and Data; Supplementary Fig. 8) and to ensure the comparability of the
158 inequality between specific sectors and food categories.

159 Grains, poultry, and pig meat were identified as the top three food types associated with the
160 highest inequality, whereas vegetables, fruits, and non-meat animal-sourced foods (eggs and dairy)
161 demonstrated minor inequality (Fig. 2 and Supplementary Table 1). The low level of inequality
162 associated with vegetables and fruits can be attributed to their smaller environmental footprint,
163 perishable nature, and difficulties in storage³⁰, thus tending to be consumed locally. When
164 considering inequality across protein types, the disparity is considerably greater for animal-sourced
165 protein than for plant-sourced protein, particularly for red meat (livestock meat, including beef, pig
166 meat, sheep and goat) and poultry (Supplementary Fig. 9), resonates with findings from previous
167 studies that assess the environmental footprint of food protein^{18,31}. In highly developed and coastal
168 provinces, the health cost of producing 1 kg of protein was significantly higher than the cost of
169 consuming 1 kg of protein (e.g., 2–9 times higher in Beijing, Shanghai, and Tianjin compared with
170 the current consumption cost; Supplementary Fig. 9, right end of the curves). The substantial
171 health inequality of animal protein primarily stems from a higher air quality-related mortality per
172 unit of animal protein consumed compared to that of plant protein (Supplementary Fig. 10).

173 We investigated the inequality of the food system between rural and urban areas (segmented by
174 each province) and at different income groups. To explore income-related inequality, we classified
175 the provinces into ten income groups based on per capita disposable income, denoted as D1 to
176 D10 in descending order (i.e., D1 is the highest income group while D10 is the lowest;
177 Supplementary Table 2; see Methods and Data). Pronounced gaps in ΔM rates exist between rural

178 and urban areas (Supplementary Fig. 11) due to the rural-urban differences in M_P and M_C rates
179 (Supplementary Fig. 12), particularly for Inner Mongolia in sheep and goat since the focus
180 production in rural area while high consumption in urban area (Supplementary Fig. 11). Depending
181 on food type, 57%–94% of the rural population is exposed to higher health risks from production
182 (Supplementary Table 3) than they should be according to their consumption, compared to only
183 0%–22% for their urban counterparts. Particularly for red meat, over 90% of the rural population
184 bears an excess health burden, compared to 0%–16% for the urban population. This is primarily
185 attributable to the substantially higher emissions exposed during production in rural areas
186 compared to urban areas (Supplementary Fig. 13).

187 M_C rates increase with income (Fig. 3a). The highest mortality rate occurred in the second highest
188 income group, D2 (2.45 deaths per 10,000 population; 95% CI, [1.59, 3.34]). However, a significant
189 decline was observed in the top income group, D1 (1.43 deaths per 10,000 population; 95% CI,
190 [1.41, 2.45]; Fig. 3a). This decline is attributed to the lowest contribution of meat consumption to
191 per-capita deaths in D1 compared to other high-income groups (D2–D5), due to their health-
192 conscious diet with lower grains and ruminant meat intake (Supplementary Table 4). In contrast,
193 M_P are generally negatively correlated with income, although the lowest income groups (D9–D10)
194 do not follow this trend due to harsh local conditions for crop growth (e.g., rural areas in Gansu,
195 Qinghai, and Tibet). Overall, low-income groups (D6–D10) experienced 70% more health damage
196 than high-income groups (D1–D5), but food consumption in the former caused 29% less health
197 damage, leading to positive ΔM rates among low-income groups, negative ΔM rates among high-
198 income groups, and net inequality over income, which is dominated by animal-based food (Fig. 3b).

199 The ΔM rate of D5 is as low as that of the highest income groups D1–D2, mainly because these
200 groups comprise urban areas in provinces with poor planting conditions (e.g., urban areas in
201 Qinghai and Shanxi), resulting in the lowest M_P rate from grains among all income groups. The
202 inherent cause of mortality rate inequality across income groups lies in the higher concentration
203 of low-income individuals residing in regions of food production, exposing them to elevated NH_3
204 emissions. This phenomenon becomes evident when examining per capita emissions
205 (Supplementary Fig. 14), where the low-income regions (D6–D10; 9.0 kg per capita) emits 2.6 times
206 more NH_3 than the high-income group (D1–D5; 3.4 kg per capita). When attributed to food
207 consumption, the contribution is relatively limited, with no significant difference observed in per

208 capita emissions between low-income (5.8 kg per capita) and high-income (6.1 kg per capita)
209 groups.

210 To trace the sources of inequality caused by food supply between income groups, we calculated
211 net ΔM by deducting the portion that achieved a balance between mutual trade across specified
212 income groups (Methods and Data). Net ΔM represents the total number of net premature deaths,
213 i.e., the overall number of premature deaths caused by one income group to another income group,
214 after subtracting the equivalent premature deaths induced by mutual food supply. The connection
215 between income and net ΔM was evident (Fig. 4a). Generally, higher income groups (D1–D5)
216 exhibit fewer net ΔM because of their limited food exports to lower income groups (D6–D10),
217 whereas the lower income groups bear greater health damage from supplying food to higher
218 income groups. Notably, D6–D8 suffered more from food supply (positive net ΔM) than the D7–
219 D10 groups (Fig. 4a, upper left), while net less health cost (negative net ΔM) is observed in D1–D4
220 (Fig. 4a, lower right). Similar results were observed across all food types (Fig. 4b), indicating that
221 high-income groups transfer the environmental externalities through interregional food trades,
222 while low-income groups bear excess health damage, regardless of food type. The grains exhibit a
223 greater proportion of net ΔM in the D8 group attributed to other income groups, suggesting that
224 D8 bears a greater burden of premature mortality from the production of grains that is consumed
225 by other income group. This trend is primarily attributed to the prevalence of major agricultural
226 provinces within the D8 income group, notably Henan, Hebei, Jilin, and Anhui (Supplementary
227 Table 2). These provinces contributed prominently to national grain production (Supplementary
228 Fig. 15b) and related NH_3 emission (Supplementary Fig. 15a), yet their consumption levels fall short
229 of their production capacities (Supplementary Fig. 15c) due to local dietary preferences
230 (Supplementary Fig. 15e) and population variance (Supplementary Fig. 15d). A substantial portion
231 of grains from these provinces is transported to other regions for consumption, resulting in a
232 noticeable net ΔM . By comparing premature mortalities resulting from self-production and
233 consumption and interregional food trade, we found that the proportion of self-production and
234 consumption increased with income (Supplementary Fig. 16 and 17). This suggests that agricultural
235 products in developed regions are primarily produced to meet local demand rather than being
236 traded on the national market for revenue. Considering all end-use sectors, we found that food
237 contributes 41.7% of the total inequality of all end-uses in China (Supplementary Fig. 18 and

238 Supplementary Table 5), being the largest among all goods and services.

239 **Intervention strategies to improve equality**

240 Based on production- (emission mitigation) and consumption-based (diet transition) scenarios
241 (Table 1), we combined and conducted 35 scenario simulations (Supplementary Table 6) to
242 investigate whether individual scenarios or their combinations designed to reduce environmental
243 pressure and health damage would yield synergistic benefits in reducing inequality.

244 Exclusively adopting production-based emission mitigation scenarios (with dietary patterns
245 unchanged) leads to a noticeable improvement in both health damage and inequality, reducing
246 SDHII by 22–35% and premature mortality by 20–44% (Fig. 5). The reduction in inequality among
247 all production-based mitigation interventions primarily stems from decreased inequality within
248 grain production (Supplementary Fig. 19).

249 The diet transition approaches (with production emission unchanged) exhibit considerable
250 variability in inequality change (ranging from –30% to +18%; Fig. 5). Scenario DT3 (minimal
251 adjustments of the current diet toward the recommended range) demonstrates a 30% decrease in
252 inequality, whereas the DT4 scenario (consuming the average of the recommended range) exhibits
253 a limited effect (6% reduction). This implies that the former is the most favorable dietary option,
254 as it is the most practical choice for policy measures involving the minimal required transition in
255 diets. The key reason for the limited effectiveness of certain dietary transition schemes (e.g., DT1
256 with maximal adjustment to the current diet) is that while reducing meat consumption contributes
257 the most to improving equality, the benefits are offset by consuming plant-based foods (such as
258 grains, vegetables, and fruits) and non-meat animal-based foods (including dairy and eggs;
259 Supplementary Fig. 20).

260 In the combined approach of emission mitigation and dietary transition, there is a marked
261 reduction in premature mortality and associated inequalities (denoted as SDHII). The adoption of
262 moderate (DT3) and stringent (DT4) dietary transitions, alongside emission reduction strategies
263 (EM1–EM6), leads to a further 12%–27% reduction in SDHII compared to individual EM1–EM6
264 measures and a concurrently decrease in mortality rates by 3–13%. Notably, the strictest
265 production (EM6) and dietary (DT4) scenarios yield the most favorable results, reducing mortalities
266 and SDHII by 55% and 62%, respectively. This underscores the synergistic potential of dual
267 interventions at production and consumption sides in enhancing health damage reduction and

268 equality in the food system. Moreover, most scenarios modestly alleviate the uneven distribution
269 of populations experiencing disproportionate health damage (Supplementary Table 7).
270 For the food production reallocation scenarios, although the premature mortalities decrease with
271 increasing reallocation degrees (Supplementary Fig. 21), inequality (SDHI) and the proportion of
272 the population experiencing disproportionate health damage increases slightly (Supplementary
273 Table 8 and Supplementary Fig. 22). This suggest that agricultural reallocation aimed at reducing
274 health damage is insufficient for alleviating inequality.
275 In addition to supply and demand-side interventions, economic policies such as taxation and
276 subsidies can complement efforts to reduce inequality. By evaluating the value of a statistical life³³
277 (Supplementary Text2), we quantified the appropriate food tax that should be implemented or
278 subsidy that should be provided in each region (Supplementary Fig. 23) and income group
279 (Supplementary Fig. 24). Our findings indicate that middle- to high-income groups (D1–D5) should
280 be subject to a 4%–14% food tax to compensate for the excess damage suffered by low- to middle-
281 income groups (D6–D10), which could cover 6%–138% of the latter’s food costs.

282 **Discussion**

283 Revealing the inequalities of health damage within the food system is crucial for understanding
284 environmental justice and achieving the United Nations Sustainable Development Goal of reducing
285 inequalities³⁴. Our findings contribute to the ongoing discussion about the health effects of food
286 systems, focusing on the equality of air-related health impacts. By linking food production and
287 consumption, we highlight the disparities and inequalities between supply and demand ends
288 across space and food types. Our findings uncover significant and disproportionate differences in
289 air pollution–related health damage per-capita. Higher geographical inequality in production than
290 consumption is observed, perhaps due to increasing agricultural intensification and resulting
291 differences in provincial agricultural emissions. Another possible reason for the smaller demand-
292 side inequality is the convergence toward regional diets over time, possibly due to the Chinese
293 government’s efforts to promote and guide healthy diets and improve living standards³⁵.
294 Our work provides a spatially resolved, food-specific analysis of health-effect inequalities within
295 the food system. We identified optimal schemes to simultaneously reduce health damage and
296 associated inequality, expanding the options available for developing and implementing dedicated
297 mitigation policies. Nevertheless, substantial obstacles and challenges need to be addressed. For

298 example, while appropriate interventions can synergistically reduce health damage and inequality
299 on a national scale (Fig. 5), a trend of mortality may not consistently align with that of equality
300 when adopting certain more sustainable interventions (e.g., food production reallocation),
301 particularly on a regional scale (e.g., the regions indicated at both ends of the curve in
302 Supplementary Fig. 11 and 22). With the expected increase in agricultural intensification,
303 concentrating food production in certain regions could widen the differential burdens of negative
304 externalities of food production among regions and populations. Identifying the leverage points
305 that balance agricultural yield, emission reduction, and equitable distribution of pollution burdens
306 presents a complex problem for policymakers. Another emerging challenge for policymakers is the
307 need for meticulous consideration of the growing importance of NH₃ in air pollution in the future.
308 Stringent controls on NO_x and SO₂ may amplify NH₃'s role in the formation of secondary
309 aerosols^{36,37}, potentially resulting in greater health impacts. Furthermore, implementing
310 diversified regulations and protocols to reduce inequality can be challenging. Our results show that
311 food consumption recommendations (e.g., self-production and marketing, or import from other
312 regions; food intake) may need to vary based on regional specifics, which could hinder the
313 development and adoption of policy-related measures, especially when coordination between
314 national and local policies is critical. Given the intricacy of food system transformation,
315 policymakers must concurrently develop short- and long-term policies to address future challenges.
316 In the short term, achieving a more equitable distribution of negative externalities in the food
317 system may not be immediately feasible, so economic measures are recommended to compensate
318 for excess health damage, such as implementing food taxes to subsidize food production regions
319 (Supplementary Fig. 23 and 24). In the long term, policymakers need to phase in top-level design
320 and restrictive policies for food system emissions and the related equality, accounting for factors
321 such as the spatial heterogeneity of health costs associated with food production, anticipated
322 dietary transitions in the local context, and nutritional requirements due to population growth, as
323 well as the overall sustainability goals pursued by the nation. Our research investigates the
324 potential synergies between health damage and inequalities (Fig. 5), providing valuable references
325 for policy development.

326 As the world's most populous country, China faces tremendous pressure on its food supply system
327 due to improved living standards. While the development of agricultural intensification and mature

328 food supply chains has satisfied the food demands, they have also led to significant food system-
329 related inequalities. It is worth noting that China is not alone in experiencing these inequalities. In
330 a follow-up first-order analysis that expands the current assessment scale, we found that countries
331 worldwide, particularly middle- and high-income countries, exhibit significant inequality in
332 agricultural NH₃ emissions exposure (Supplementary Text3, Supplementary Fig. 25). This
333 observation indicates that countries with more advanced food systems may encounter greater
334 challenges relating to agricultural emissions and associated inequalities. Our study illuminates the
335 issue of food system inequality, offers valuable guidance for policymakers in China while also serves
336 as a point of reference for the sustainable development of food systems worldwide.

337 **Methods**

338 We developed a comprehensive modeling framework to estimate the health damage due to PM_{2.5}
339 pollution exposure from the food system in China and analyzed the associated health damage
340 inequality (Supplementary Fig. 26). The development of the framework includes several steps.
341 Initially, the atmospheric emissions from the supply and demand sides of the food system were
342 linked using the Multi-Regional Input–Output (MRIO) model³⁸. Then, we used the Global Exposure
343 Mortality Model (GEMM)³⁹ to estimate premature mortality associated with ambient PM_{2.5}
344 exposure and the sensitivities of premature mortality to ambient PM_{2.5} concentrations by grid cell.
345 Subsequently, we coupled the concentration sensitivities into multiphase Adjoint for the
346 Community Multiscale Air Quality (CMAQ-Adjoint) model²⁶ to compute the sensitivities of
347 premature mortality to emissions. These matrices encompass all pollutant species, locations, and
348 time, allowing us to estimate their relative contributions on both the supply and demand sides. To
349 analyze inequality, we developed an index, SDHII, to quantify the national inequality pattern in the
350 gap between PM_{2.5}-related premature mortality associated with food supply and demand. The
351 detailed procedures are described in the following sections.

352 **Atmospheric emissions from food production to consumption**

353 We initiated our study by developing a production-based emission inventory of all the production
354 sectors of China in 2017, for which the global high-resolution emission inventory product (10 km ×
355 10 km) published by Peking University (PKU-Inventory) for atmospheric emissions across sectors
356 (e.g., power generation, industry, transportation, and agriculture), fuel types (e.g., coal, oil, natural
357 gas, and biomass), and pollutants (e.g., primary PM_{2.5}, SO₂, NO_x, CO, OC, BC) was used²²⁻²⁵. Note

358 that PKU-Inventory also includes NH₃ emissions from non-agricultural activities²¹. Additionally, a
359 Chinese agricultural emission inventory with 1 km × 1 km resolution developed by Adalibieke et
360 al.¹⁹ (crop NH₃ volatilization) and Wang et al.²⁰ (livestock management) was employed to calculate
361 the NH₃ emissions associated with agricultural activities. This comprehensive inventory covered
362 NH₃ emissions from the production of nine food categories, including grains, vegetables, fruits, pig
363 meat, beef, sheep and goat, poultry, dairy, and eggs. The emissions from dairy and egg products
364 considered in this study arise from the rearing processes of dairy cows and egg-laying hens. Due to
365 a portion of grains being used for animal feed, we reallocated the NH₃ emissions from this feed
366 portion to animal-sourced food. Using food consumption data of China extracted from the United
367 Nations FAOSTAT database⁴⁰, we computed that in 2017, approximately 32% of grains was used for
368 livestock feed in China. This proportion closely resembles the results of Liu et al., 2021 (34% in
369 2010)⁴¹. Subsequently, we redistributed the emissions from this portion of grains based on the NH₃
370 emission proportions of different animal-based food sources. By integrating this food emission
371 inventory into the PKU-Inventory, we expanded the current inventory to provide a detailed account
372 of agricultural emissions. Subsequently, we reallocated all the atmospheric pollutants according to
373 provinces to align them with the production sectors in the MRIO models using Energy Balance
374 Sheets from the China Energy Statistical Yearbook⁴². The resulting provincial production-based
375 emission inventory comprised 42 production sectors (Supplementary Table 9) corresponding to the
376 MRIO production sectors of the nine food categories.

377 To establish a link between pollutant emissions between the food supply and demand sides, we
378 employed Environmental Extended Input–Output Analysis (EEIOA) to create a consumption-based
379 emission inventory. EEIOA is an extended application of input–output analysis that enables the
380 explicit analysis of environmental impacts⁴³. Initially, we employed traditional economic
381 accounting, expressing the input–output link function as Eq. (1):

$$382 \quad X = (I - A)^{-1}Y \quad (1),$$

383 where X represents the economic output matrix, A is a normalized matrix of intermediate
384 coefficients where columns correspond to the input required from sectors in a given region to
385 produce one unit of the output of each sector in another region, $(I - A)^{-1}$ is the Leontief inverse
386 matrix, and Y is a vector of the finished consumption. Subsequently, we incorporated emission
387 information using Eq. (2):

388 $E = f(I - A)^{-1}Y$ (2),

389 where E represents atmospheric emissions embedded in flows of goods and services between the
 390 sectors. The matrix f is diagonal, with emission intensities (emissions for unit output) for each
 391 sector along the diagonal and zeros in all the other positions.

392 A consumption-based emission inventory (referred to as S) was generated using EEIOA that
 393 illustrates how emissions are embodied in the flows of goods and services among the production
 394 sectors, ultimately reaching the final consumption sectors. This inventory includes 31 provincial-
 395 level administrative divisions (excluding Taiwan, Hong Kong, and Macao, as data for these regions
 396 were unavailable), 42 production sectors, and 5 consumption sectors.

397 The consumption-based emission inventory quantifies virtual emission flows specific to each
 398 region, spanning from supply to demand sides. Subsequently, we calculated the emissions
 399 attributed to production (E_p) and consumption (E_c) at the provincial level using Eq. (3) and (4):

400 $E_p = \sum_c S$ (3)

401 $E_c = \sum_p S$ (4),

402 where S represents the consumption-based inventory; p and c is the supply and demand sides of
 403 the inventory, respectively; E_p is a transposed matrix of $(E_p^1 \ E_p^2 \ E_p^3 \ \dots \ E_p^Q)$, where E_p^i
 404 represents the production-based emissions in a given province i , and Q is the total number of
 405 administrative divisions (31 in this study, excluding Hong Kong, Macao, and Taiwan due to data
 406 limitations). Similarly, E_c is a transposed matrix of $(E_c^1 \ E_c^2 \ E_c^3 \ \dots \ E_c^Q)$, where E_c^i denotes
 407 the consumption-based emissions in a given province i .

408 Next, we computed the relative contribution of emissions for each province at both the supply and
 409 demand ends, denoted as:

410 $r_{i,j} = \frac{S_{i,j}}{\sum_{c=1}^Q S_{i,c}}$ (5),

411 where $r_{i,j}$ represents the relative share of emissions within a given region i at the supply side,
 412 concerning region j at the consumption end. To consolidate all relative shares of emissions along
 413 the supply chain, we employed the matrix R , defined as:

414 $R = \begin{pmatrix} r_{1,1} & \dots & r_{1,Q} \\ \vdots & \ddots & \vdots \\ r_{Q,1} & \dots & r_{Q,Q} \end{pmatrix}$ (6),

415 where R incorporates all the relative shares of emissions.

416 To appropriately allocate agricultural emissions within the food supply chain, we applied a double
417 constraint to this portion of the emissions. First, we extracted the economic flow from the
418 agricultural sectors to the rural and urban consumption sectors, as generated by the MRIO model.
419 Next, we redistributed the food emissions of each province by (1) calculating the relative share of
420 monetary flows from each province on the demand side to provinces on the demand side, yielding
421 a supply-side constraint matrix (labeled as H_1); (2) determining the total amount of annual per-
422 capita food consumption in 2017 for each food type using data from the Chinese National Bureau
423 of Statistics⁵; and (3) matching the total food consumption to that of each province in the demand
424 side and redistributing it according to H_1 . These steps ensured that the relative proportions of each
425 food type in the supply side for a given province were adequately constrained. Each food type was
426 individually distributed on the demand side based on the scaling factors.

427 To ensure that the total amount of emissions was conserved for each food type from the supply to
428 demand side, we calculated the relative share of the amount of food in the aforementioned result
429 for each province on the supply side as an emission-constraint matrix (labeled as H_2). Subsequently,
430 we redistributed agricultural emissions from the supply side to the demand side using H_2 . Notably,
431 we did not conduct a detailed analysis of the residential sectors because the overall estimation
432 framework is based on the reclassification of the production sectors. Nevertheless, we treated this
433 part as a whole and accounted for it when evaluating the contribution of each component to the
434 premature mortality⁴⁴.

435 **Health damage estimation**

436 The latest version of the CMAQ-Adjoint, version 5.0, was utilized in our study to quantify the
437 contributions of location-, time-, and pollutant-specific emissions to premature mortality. CMAQ-
438 Adjoint is comprised of two models: a forward model, which mirrors the original CMAQ base model,
439 and a backward model. We applied CMAQ-Adjoint to a geographical domain encompassing East
440 Asia, defined by 124×184 horizontal grid cells at a resolution of 36 km, and 13 vertical layers
441 extending to approximately 16 km above ground. For evaluation, a 1-year simulation using the
442 CMAQ base model was conducted. The results have been illustrated in a previous study, indicating
443 a general concordance with observed spatial distributions and temporal trends of multiple
444 pollutants.

445 The backward model allowed us to calculate sensitivities, that is, the partial derivatives of the

446 objective function concerning related input parameters. By defining the objective function J as the
 447 total premature mortality from ambient PM_{2.5} exposure within China in 2017, we incorporated the
 448 GEMM into the adjoint analysis. The objective function J was expressed by the following equations,

$$449 \quad J = \sum M_{0,x,y} P_{x,y} [1 - e^{-\theta T(z_{x,y})}] \quad (7)$$

$$450 \quad T(z_{x,y}) = \frac{\log(1 + \frac{z_{x,y}}{\alpha})}{1 + e^{-\frac{-(z_{x,y} - \mu)}{\nu}}} \quad (8)$$

$$451 \quad z_{x,y} = \max(0, C_{x,y} - cf) \quad (9)$$

452 where (x, y) denotes a specific model grid cell; $M_{0,x,y}$ represents the baseline mortality rate at grid
 453 cell (x, y) ; $P_{x,y}$ represents the population within grid cell (x, y) ; $C_{x,y}$ denotes the location-specific
 454 annual PM_{2.5} concentration at grid cell (x, y) , in $\mu\text{g}\cdot\text{m}^{-3}$; cf is the concentration threshold below
 455 which no health association is assumed to be identifiable. The term $1 - e^{-\theta T(z)}$ is the GEMM
 456 equation to calculate the population-attributable fraction (PAF)³⁹. As suggested by Burnett et al.³⁹,
 457 the following values for the GEMM parameters were used to calculate PAF of noncommunicable
 458 diseases and lower respiratory infections (NCD+LRI) mortality from ambient PM_{2.5} exposure for
 459 adults aged 25–99: $\theta = 0.1430$, $\alpha = 1.6$, $\mu = 15.5$, $\nu = 36.8$, $cf = 2.4 \mu\text{g}\cdot\text{m}^{-3}$. $M_{(x,y)}$ is determined by the
 460 baseline mortality rate of NCDs+LRIs of the province where (x, y) is located⁴⁵. Further details
 461 regarding the parameter configuration of GEMM can be found elsewhere³⁹.

462 We then derived the adjoint forcing term using Eq. (10),

$$463 \quad \varphi_{x,y} = \frac{\partial J}{\partial c_{x,y}} = M_{0,x,y} P_{x,y} \theta e^{-\theta T(z_{x,y})} T'(z_{x,y}) \frac{dz_{x,y}}{dc_{x,y}} \quad (10)$$

464 where $\varphi_{x,y}$ is the adjoint forcing at grid cell (x, y) ; $c_{x,y}$ denotes the PM_{2.5} concentration at grid cell
 465 (x, y) at any time step; $dz_{x,y}/dc_{x,y}$ is equal to the reciprocal of the number of model time steps in a
 466 year and is set to 1/43800 in our simulation (12 minutes per time step); $T'(z_{x,y})$ is the derivative of
 467 $T(z)$ at $z = z_{x,y}$. In the adjoint simulation, these forcing terms were applied to all modeled PM_{2.5}
 468 species as inputs to derive the adjoint sensitivities of mortality to location- and time-specific
 469 emissions of primary PM_{2.5} and precursors. Similar assessment has been conducted in our CMAQ-
 470 adjoint development paper²⁶. It should be noted that the computational expense of running the
 471 CMAQ-Adjoint model is about fourteenfold compared to the base CMAQ model. A single-day
 472 simulation using the CMAQ-Adjoint model, encompassing both forward and backward simulations
 473 in our study domain, on average necessitates 2.2×10^5 seconds of CPU time. Extrapolating this to
 474 the one-year timeframe of our study, the cumulative CPU time approximates 8.2×10^7 seconds,

475 translating to roughly 950 days.

476 We extracted the premature mortalities (i.e., the number of deaths before reaching their life
477 expectancy) from the production sectors related to the food system using the adjoint sensitivities.

478 The premature mortalities specified by production sectors were then linked to the consumption
479 sectors of both rural and urban residents based on the input–output analysis. This process yielded
480 a dataset of PM_{2.5}-related health damage for the entire food system, facilitating further analysis of
481 inequality. In contrast to previous methods that directly calculate sector and species contributions
482 using the objective function in the production or emission sector⁴⁶⁻⁴⁸, our approach establishes a
483 connection between mortality, production, and consumption sectors within the food system based
484 on the consumption-based emission inventory.

485 **Inequality evaluation in premature mortality related to PM_{2.5} exposure**

486 We introduced SDHI to evaluate the inequality in air quality-related health damage attributed to
487 the food system. This index considers the disparity in mortality rates between production- and
488 consumption-based accountings in each province. By population weighting, it quantifies the
489 inequality in mortality rates between production and consumption at the national level. The more
490 intuitive explanation of this index is visualized in Supplementary Fig. 8. The calculation process
491 comprises two steps.

492 First, we calculated the disparity between premature mortalities attributed to food production (M_P)
493 and consumption (M_C) for each province, which is denoted as ΔM^i and represents the difference
494 in health damage incurred in a region owing to local food production versus the health damage
495 expected from local food consumption within the same region (accounting for local and nonlocal
496 food sources). Mathematically, it is defined by Eq. (11):

$$497 \quad \Delta M^i = M_P^i - M_C^i \quad (11),$$

498 where M_P^i and M_C^i represent the M_P rate (deaths per 10,000 population) in the supply side (i.e.,
499 province i supplies food to other regions) and the M_C rate (deaths per 10,000 population) in the
500 demand side (i.e., province i receives food from other provinces) for a given province i .

501 The ΔM rates represent the level of balance between the M_P and M_C rates with the food system.
502 When the mortality rates from regional food production and consumption are balanced, ΔM equals
503 zero. If ΔM^i is >0 for a specific province, it indicates that the region experiences an excess number

504 of deaths owing to its food supply to other regions. These provinces are referred to as “production-
505 oriented,” while provinces with lower health damage ($M_C > M_P$) are labeled as “consumption-
506 oriented.”

507 Next, we ranked all the ΔM rates in ascending order and paired them with population data from
508 each region (Supplementary Fig. 8a), following which the SDHII was computed using Eq. (12):

$$509 \quad SDHII = \frac{\sum_{i=1}^n POP_i \times |M_P^i - M_C^i|}{POP} \quad (12),$$

510 where POP and POP_i represent the national population and population for a given province i ,
511 respectively, and n denotes the total number of provinces.

512 Intuitively, SDHII corresponds to the area depicted in Supplementary Fig. 8b. This index represents
513 the level of national-scale inequality in health damage. It incorporates population proportion as a
514 weighting factor and captures the regional disparities arising from food production and
515 consumption. When the health damage experienced by a particular region aligns with the expected
516 damage based on food consumption, the ΔM rates for that region are zero, indicating no
517 contribution to SDHII. In an ideal scenario, each region bears health damage proportionate to its
518 consumption, resulting in a balanced distribution of premature mortalities and an SDHII value of 0.

519 To trace the manifestation of health damages across different income groups, we employed the
520 provincial income data obtained from the National Bureau of Statistics of China⁵ to categorize all
521 provinces into ten income groups. Given that the income dataset distinguishes between urban and
522 rural residents for each province, we further classified each province into two population subsets:
523 urban and rural. Consequently, this resulted in a total of 62 distinct population subsets across 31
524 provinces/regions under consideration. These population subsets were subsequently assigned to
525 ten income groups, with each group comprising six population subsets, except for the lowest
526 income group which comprised ten subsets (Supplementary Table 2). The division of the income
527 groups is illustrated in Supplementary Fig. 27. Next, we conducted pairwise matching among the
528 income groups and calculated the difference in health damage resulting from reciprocal food
529 supply between them, enabling us to evaluate the net premature mortality caused by the
530 intergroup food supply, which is denoted as net ΔM , and can be expressed by:

$$531 \quad \text{net } \Delta M^{i,j} = \Delta M^{i,j} - \Delta M^{j,i} \quad (13),$$

532 where net $\Delta M^{i,j}$ represents the net premature mortality between the selected income group i and

533 another given income group j . This metric evaluates the net health damage between the different
534 income groups after offsetting the respective health damage associated with food consumption. If
535 net $\Delta M^{i,j}$ is >0 , the income group j causes excess health damage to the income group i and gains
536 health benefits from food trade owing to the food supply from i to j . Conversely, if net $\Delta M^{i,j}$ is <0 ,
537 the group j experiences more health damage because of the food supply to the group i .

538 **Intervention strategies**

539 We investigated the potential cobenefits of reducing inequality from various intervention
540 approaches aimed at reducing emission or developing a balanced diet. We designed three
541 intervention scenarios: agricultural emission mitigation, diet transition, and agricultural production
542 reallocation. Each scenario includes several subscenarios that differ in implementation intensity,
543 feasibility, and expected benefits (Table 1).

544 We conducted six subscenarios to mitigate agricultural NH_3 emissions, comprising four single and
545 two collaborative measures, as outlined by Kang et al.³² and Adalibieke et al.¹⁹. The “Intergrated
546 NH_3 reduction strategies” (EM1) scenario involves the incorporation of reduced fertilizer application,
547 deep fertilizer placement, and the use of a urease inhibitor. In the “Increasing mechanized deep
548 fertilization” (EM2) scenario, the incorporation proportion of synthetic N fertilizers is set to reach
549 80% for wheat, maize, and rice based on the National Agriculture Mechanization Extension Plan⁴⁹.
550 In the “Optimizing fertilizer types” (EM3) scenario, we assumed that 50% of N applications were
551 allocated to organic fertilizer and manure for major crops, vegetables, and fruits⁴⁹. In the
552 “Optimizing fertilizer rates” (EM4) scenario, the N fertilizer rate was reduced to meet the “N Surplus
553 Benchmarks” in seven regions, as proposed by Zhang et al.⁵⁰ and the European Union Nitrogen
554 Expert Panel⁵¹. The regional “N Surplus Benchmarks” were utilized as the targeted N surplus in
555 regions where the N surplus exceeds the benchmarks.

556 For the diet transition scenario, we explored the potential for reducing inequality by adopting
557 healthier dietary habits. Our dietary recommendations were based on the 2022 Chinese Dietary
558 Guidelines (CDG 2022). The scenario considered nine food categories: grains, vegetables, fruits, pig
559 meat, beef, sheep and goat, poultry, dairy, and eggs. Using CDG 2022 as a reference, we designed
560 four subscenarios for the entire population, balancing healthfulness and feasibility to varying
561 degrees. The four subscenarios included (1) adjusting food intake for each category to the upper
562 limit of the recommended range in CDG (DT1); (2) adjusting food intake for each category to the

563 lower limit of the recommended range in CDG (DT2); (3) adjusting food intake for each category
564 based on the minimum difference between the existing diet and the recommended range (DT3);
565 and (4) adjusting food intake for each category to the average values of the recommended range
566 in CDG (DT4). For example, if the current food intake exceeded the upper limit of the recommended
567 range, it was adjusted to the upper limit range. Conversely, if the intake was below the lower limit,
568 it was adjusted to the lower limit. No adjustments are made if the current intake is already within
569 the recommended range. We computed the percentage of changes in food intake owing to the
570 dietary transition of each food category, which formed the diet transition matrix (labeled as H_3),
571 based on which we recalculated the premature mortality for each food category in each province
572 to represent the changes in health damage and equality for each subscenario.

573 Agricultural production reallocation aimed to mitigate health damage by redistributing crop
574 production from high- to low-sensitivity areas. Certain regions are more susceptible to $PM_{2.5}$
575 emission, leading to more premature deaths per production unit than other regions. Herein, we
576 assumed a fixed spatial distribution of farmlands to avoid potential environmental footprints
577 related to alterations in land use, such as new farmland cultivation^{7,52}. Thus, we analyzed crop
578 reallocation by transferring production from farmlands with high $PM_{2.5}$ sensitivity to existing
579 farmlands with $PM_{2.5}$ sensitivity while maintaining crop yield. This transfer of crop yield from high-
580 to low-sensitivity areas requires a certain level of yield increase in those low-sensitivity regions.
581 While concentrating crop production in the areas with the lowest sensitivity would ideally
582 maximize health benefits, it is impractical owing to the limited production potential. We assumed
583 a 30% yield increase in each crop production area and a maximum reduction of 20% in the total
584 crop production in high-sensitivity areas considering the yield ceiling in low-sensitivity areas.
585 Consequently, we designed 20 subscenarios to transfer production from regions with higher
586 mortality rates per unit production (1%–20% of the total production) to regions with lower
587 mortality rates. First, we calculated the mortality rate per unit of crop production for each province
588 using data from the Chinese National Bureau of Statistics⁵. Then, starting with the province with
589 the highest mortality rates (province A), we transferred crop yield to the province with the lowest
590 mortality rates (province B) until the yield increase in province B reached 30% of its initial crop
591 yield. This process was repeated for the second-best province and continued until the total
592 transferred production yield reached 20%. We achieved the desired reallocation by sequentially

593 allocating transferred yields to regions with the lowest mortality rates per unit.

594 We conducted an assessment of uncertainty and analyzed limitations for our study. Refer to the

595 Supplementary Information for details.

596

597 **Data availability**

598 The data supporting the findings of this study are available within the article and Supplementary

599 Information. Population, residents' disposable income, and food intake data at the site scale from

600 the National Bureau of Statistics of China are available at <http://data.stats.gov.cn/>. China Multi-

601 Regional Input–Output Table is available at http://www.ceads.net/data/input_output_tables/.

602 Livestock feeding data is derived from <https://www.fao.org/faostat/>. Source data for premature

603 mortalities is accessible on Zenodo: <https://doi.org/10.5281/zenodo.10645774>.

604

605 **Code availability**

606 Python 3.8 was used for developing the Environmental Extended Input–Output Analysis (EEIOA)

607 and for data analysis. The source codes utilized in this study can be accessed on Zenodo:

608 <https://doi.org/10.5281/zenodo.10645774>.

609

610 **Acknowledgements**

611 G.S. and H.S. acknowledge funding from Ministry of Science and Technology of the People's

612 Republic of China (2023YFE0112900). H.S. acknowledges funding from the National Natural

613 Science Foundation of China (42192510). F.Z. acknowledges funding from the National Natural

614 Science Foundation of China (42225102). S.T. acknowledges funding from the National Natural

615 Science Foundation of China (41991312, 41821005, and 41830641). T.-M.F. and H.S. acknowledge

616 funding from Shenzhen Science and Technology Program (JCYJ20220818100611024). G.S.

617 acknowledges funding from the National Natural Science Foundation of China (42077328). X.Y., T.-

618 M.F., and H.S. acknowledge funding from the Shenzhen Key Laboratory of Precision Measurement

619 and Early Warning Technology for Urban Environmental Health Risks (ZDSYS20220606100604008),

620 Department of Science and Technology of Guangdong Province (2021B1212050024), and

621 Department of Education of Guangdong Province (2021KCXTD004). H.S. acknowledges support

622 from Center for Computational Science and Engineering at Southern University of Science and
623 Technology.

624

625 **Author contributions**

626 H.S., J.M., P.H., and F.Z. conceived and initiated the study. L.Z. and W.A. processed and analyzed
627 the data. Y.C., P.G., J.H., and Y.Z. provided support with data collection and processing. P.X., C.W.,
628 J.Y., and L.Z. assisted in the development of the model framework. L.Z. drafted the manuscript, and
629 G.S., T.-M. F., and X.Y. participated in the result discussions. H.S., F.Z., J.M., P.H., S.Z., A.H., S.T., and
630 A.G.R. provided critical revisions.

631

632 **Competing interests**

633 The authors declare no competing interests.

634

635 **Tables**

636 **Table 1 | Description of designed scenarios.** EM1 is developed by Kang et al.³², which incorporates
637 the implementation of reduced fertilizer application, deep fertilizer placement as well as the use
638 of a urease inhibitor; EM2–6 are developed by Adalibieke et al.¹⁹.

Scenario	Sub-scenario	Description
BAU		Business-as-usual
Emission mitigation	EM1	Intergrated NH ₃ reduction strateges
	EM2	Increasing mechanized deep fertilization
	EM3	Optimizing fertilizer types
	EM4	Optimizing fertlizer rates
	EM5	Integrating EM2 and EM3
	EM6	Integrating EM2, EM3 and EM4
Diet transition	DT1	Adhering to the maximum recommended food intake in the 2022 Chinese Dietary Guidelines (CDG)
	DT2	Adhering to the minimum recommended food intake in the 2022 CDG
	DT3	Minimum adjustments to resident’s diet based on the 2022 CDG
	DT4	Adhering to the average recommended food intake in the 2022

639

Figure Captions**Fig. 1 | Provincial-level distributions and inequalities of premature mortalities due to food**

production and consumption in China. Annual premature mortality rates from (a) food production (M_P rates) and (b) food consumption (M_C rates). (c) Difference between M_P rates and M_C rates (ΔM rate). (d) The Gini coefficients of M_P rates and M_C rates. The provincial boundary shapefile has been obtained from Harvard Dataverse (<https://doi.org/10.7910/DVN/DBJ3BX>) and is publicly available under the Creative Commons CC0 Public Domain Dedication.

Fig. 2 | Inequality within the food system across food types. Shown are ΔM rates (difference in mortality rates attributable to $PM_{2.5}$ exposure from food production versus consumption) of each province, sorted in ascending order. The provinces with ΔM mortality rates >0 (on the right side of the curves) are “production-oriented” provinces, indicating that the mortality from local food production surpass that attributed to food consumption. Conversely, if the ΔM rates are <0 (i.e., “consumption-oriented” provinces), the opposite holds true. The inequalities are quantified as the Supply–Demand Health Inequality Index, indicated in parentheses in the legend for each food type.

Fig. 3 | Mortality disparity across income groups. (a) Relationship between income and premature mortality, including premature mortality rates attributed to food production (M_P rates) and consumption (M_C rates). We sorted all provinces based on residents’ disposable income and categorized them into ten income groups in descending order (D1–D10; Methods and Data). The shading indicates the range between the 25th and 75th percentiles. (b) Mortality rate differences attributable to $PM_{2.5}$ exposure from food production vs. consumption (ΔM per 10,000 population) by income decile. The impacts of various food types on ΔM rates differ among income groups, with each type contributing positively or negatively. The net ΔM rates are presented as black dots.

Fig. 4 | The net gap of premature mortalities between production and consumption (net ΔM) is shown for each pair of income groups. Net ΔM in each cell indicates the gap of premature mortality after deducting the equivalent mortality due to mutual food supply for a given pair of income groups. This result represents the attribution of mortality responsibilities in two specified

668 regions after considering the balance between production and consumption. All provinces in China
669 were classified into ten income groups based on residents' disposable income in 2017⁵, denoted
670 as D1–D10, representing income groups in descending order (i.e., D1 is the highest income group;
671 see Methods and Data). As each region is simultaneously a food supplier and consumer, we defined
672 "R1" and "R2" to establish the direction for statistical and visual purposes. If the number of deaths
673 is positive, the group in "R1" caused a net ΔM toll suffered by "R2," while negative means the
674 opposite. For instance, the positive result in the cell at the intersection of row D7 and column D3
675 indicates that more health damage is incurred on D7 by D3 in mutual supply. Seven food types
676 were considered, namely, grains, vegetables, fruits, pig meat, beef, sheep and goat, poultry, dairy,
677 and eggs. The overall attribution of net ΔM is visible in (a), while the details for different food types
678 are presented in (b).

679 **Fig. 5 | The changes in the food system inequality and premature mortalities in response to**
680 **different intervention strategies.** We considered emission mitigation and diet transition here. Each
681 scenario includes specific sub scenarios to reflect the impacts of different intervention intensities
682 on inequality, which are pairwise to present the results of combined measures (Table 1). Scenarios
683 solely considering the production-side (excluding diet transition) are represented on the column
684 for "BAU." Meanwhile, scenarios considering only diet transition are represented on the row for
685 "BAU." Inequality is represented using the SDHI, indicated by color in the graph, while premature
686 mortalities is represented by the size of bubbles. The bubble in the bottom left corner corresponds
687 to the business-as-usual scenario, where no adjustments are made to both production- and
688 consumption-side.
689

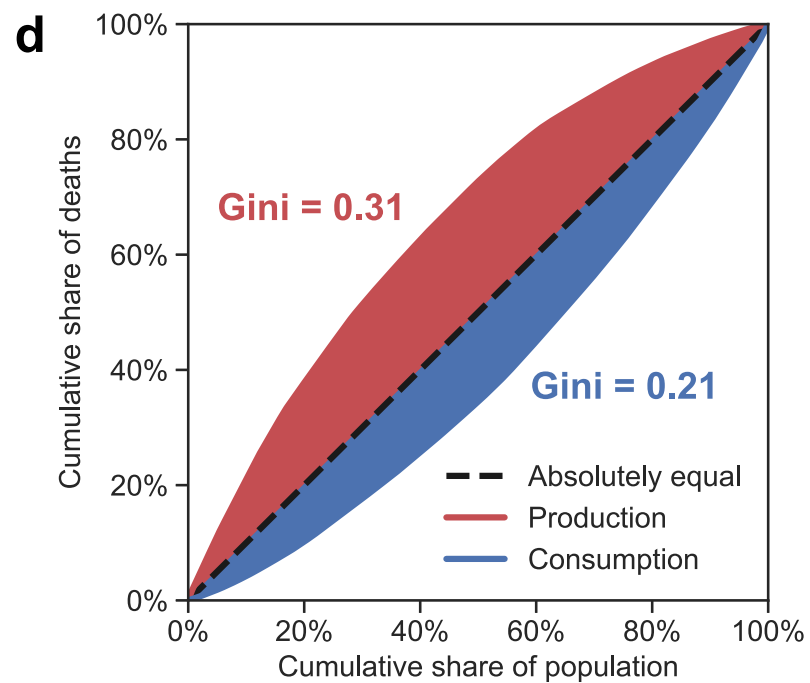
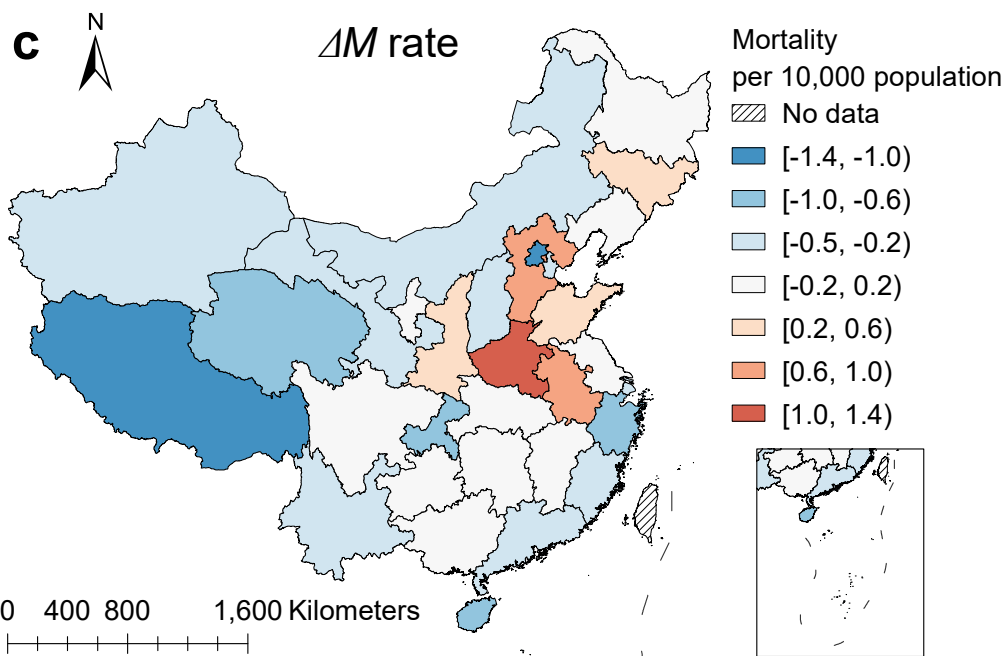
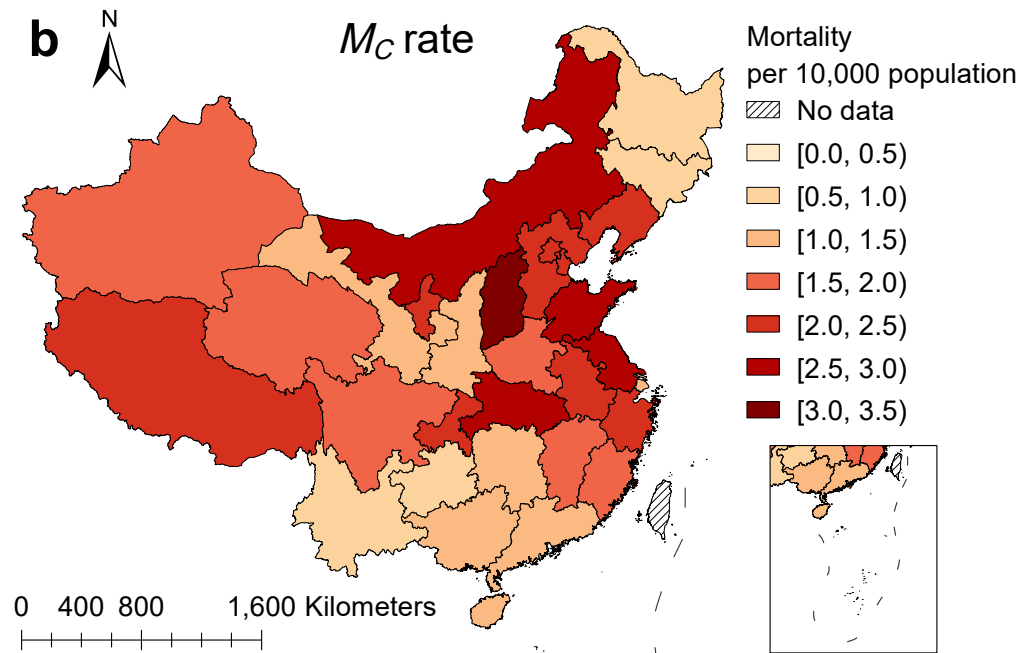
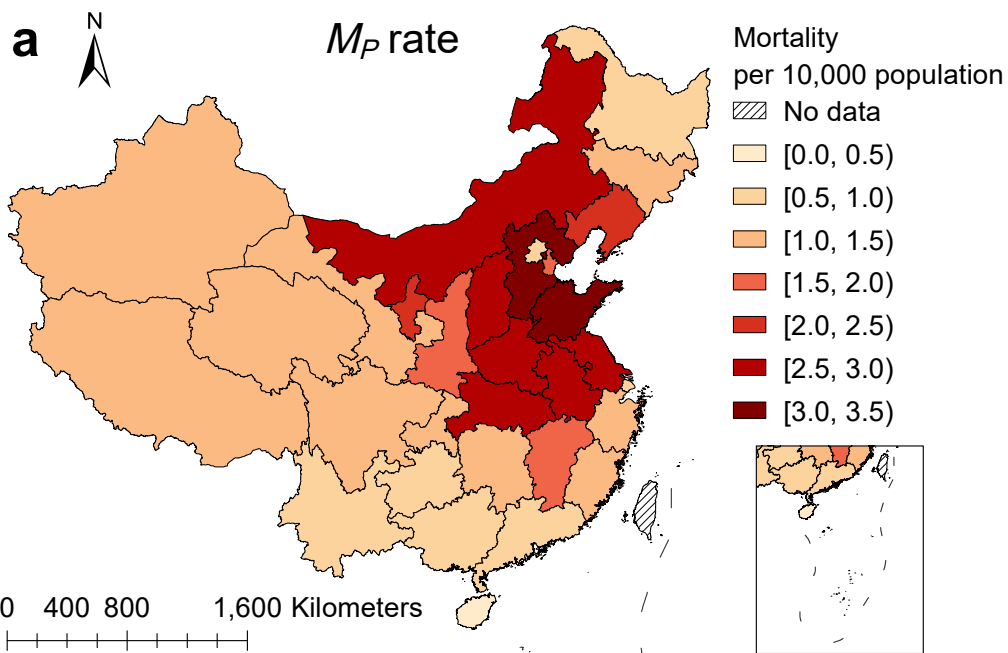
690

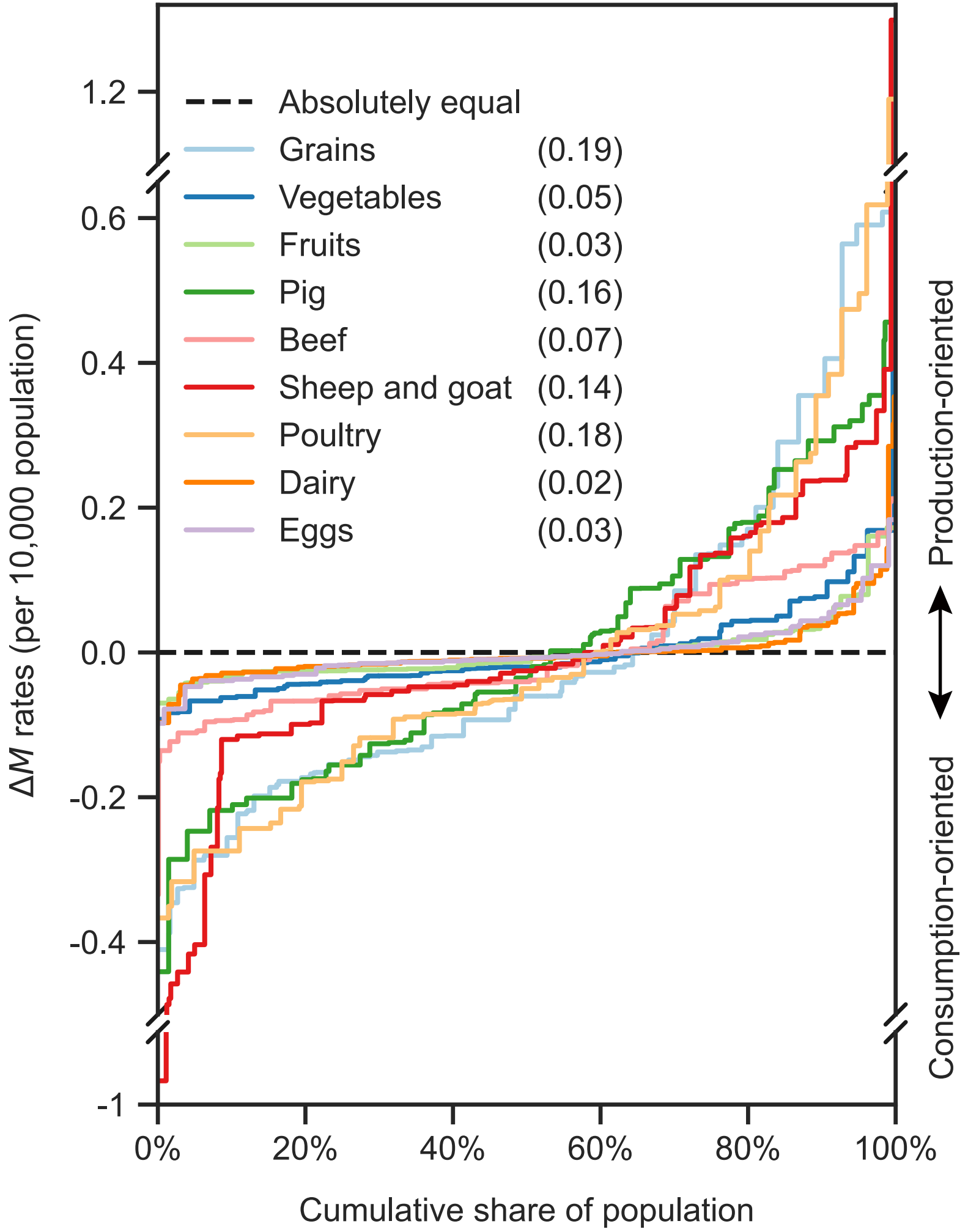
References

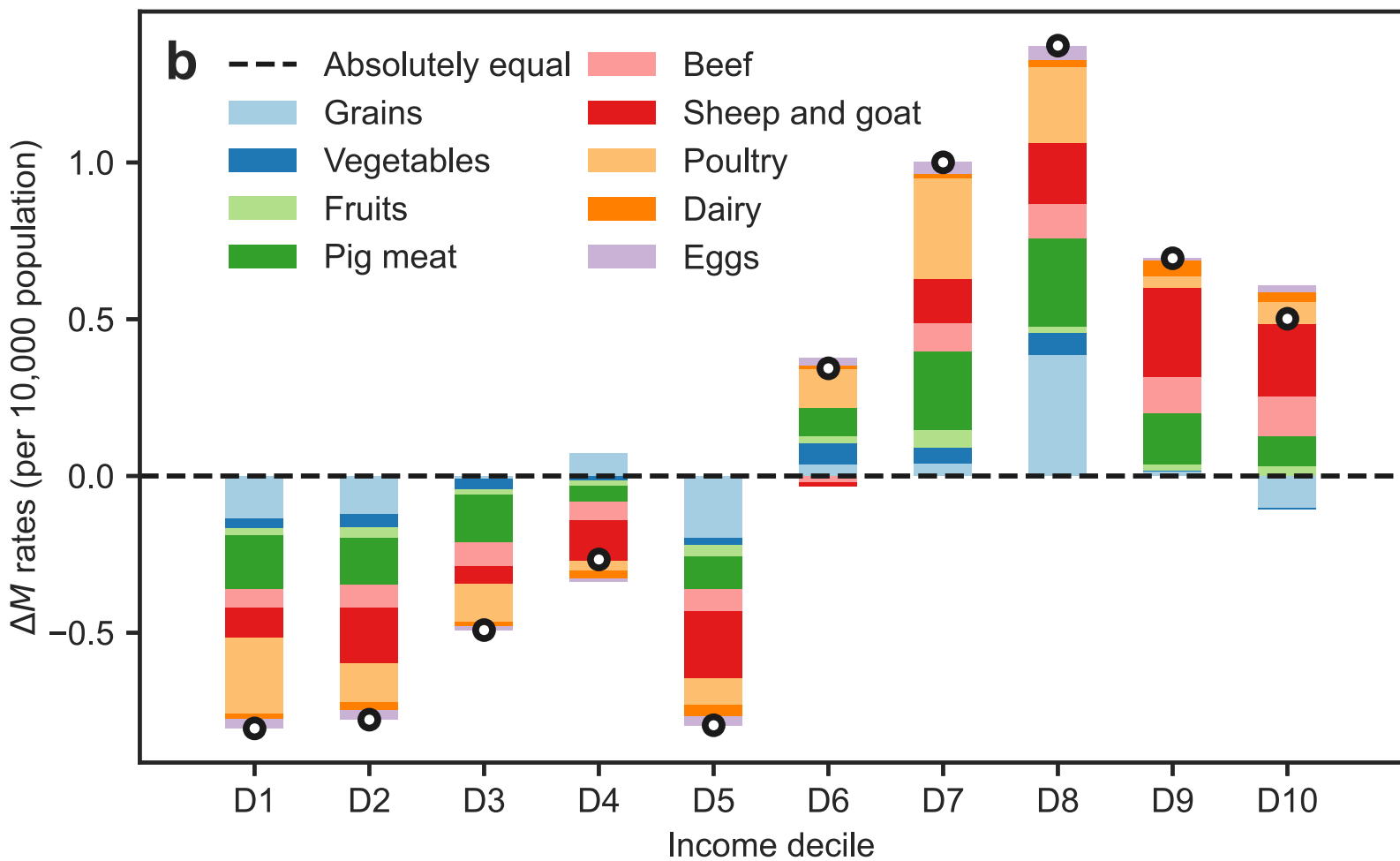
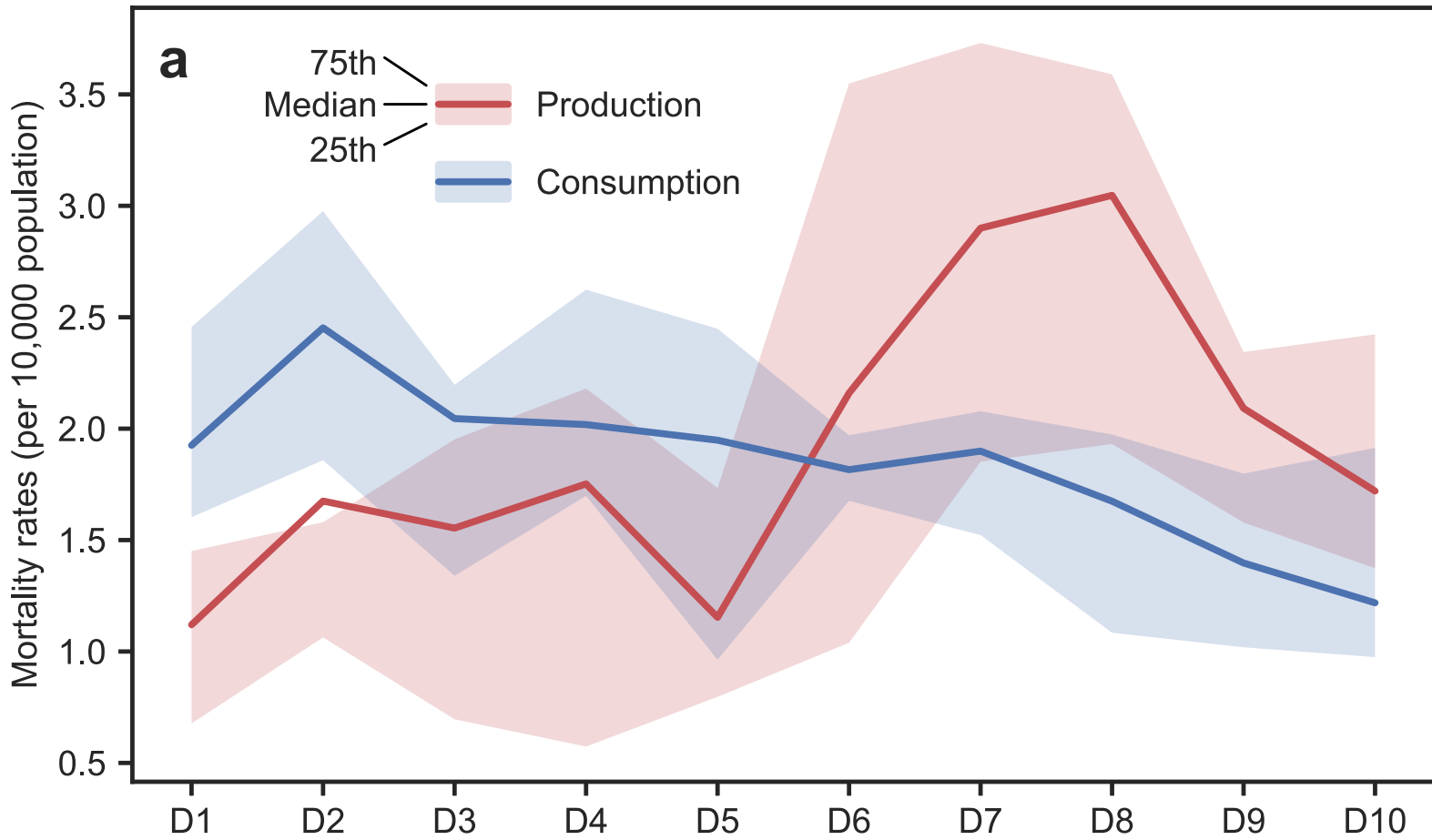
- 691 1. Rudel, T. K. et al. Agricultural intensification and changes in cultivated areas, 1970–2005.
692 *Proceedings of the National Academy of Sciences* **106**, 20675–20680 (2009).
- 693 2. Bentham, J. et al. Multidimensional characterization of global food supply from 1961 to 2013. *Nature*
694 *Food* **1**, 70–75 (2020).
- 695 3. Kinnunen, P. et al. Local food crop production can fulfil demand for less than one-third of the
696 population. *Nature Food* **1**, 229–237 (2020).
- 697 4. Huang, X. et al. A high - resolution ammonia emission inventory in China. *Global Biogeochemical*
698 *Cycles* **26** (2012).
- 699 5. NBS. *China Statistical Yearbook 2017* (China Statistics Press, 2018).
- 700 6. Tessum, C. W. et al. Inequity in consumption of goods and services adds to racial–ethnic disparities
701 in air pollution exposure. *Proceedings of the National Academy of Sciences* **116**, 6001–6006 (2019).
- 702 7. Foley, J. A. et al. Solutions for a cultivated planet. *Nature* **478**, 337–342 (2011).
- 703 8. Chen, X. et al. Producing more grain with lower environmental costs. *Nature* **514**, 486–489 (2014).
- 704 9. Springmann, M. et al. Options for keeping the food system within environmental limits. *Nature* **562**,
705 519–525 (2018).
- 706 10. Gu, B. et al. Cost-effective mitigation of nitrogen pollution from global croplands. *Nature* **613**, 77–84
707 (2023).
- 708 11. Godfray, H. C. J. et al. Meat consumption, health, and the environment. *Science* **361**, eaam5324
709 (2018).
- 710 12. Poore, J. & Nemecek, T. Reducing food’s environmental impacts through producers and consumers.
711 *Science* **360**, 987–992 (2018).
- 712 13. Hasegawa, T., Havlík, P., Frank, S., Palazzo, A. & Valin, H. Tackling food consumption inequality to
713 fight hunger without pressuring the environment. *Nature Sustainability* **2**, 826–833 (2019).
- 714 14. Clark, M. et al. Estimating the environmental impacts of 57,000 food products. *Proceedings of the*
715 *National Academy of Sciences* **119**, e2120584119 (2022).
- 716 15. Halpern, B. S. et al. The environmental footprint of global food production. *Nature Sustainability* **5**,
717 1027–1039 (2022).
- 718 16. Carter, C. A. China’s agriculture: Achievements and challenges. *ARE Update* **14**, 5–7 (2011).
- 719 17. Lam, H.-M., Remais, J., Fung, M.-C., Xu, L. & Sun, S. S.-M. Food supply and food safety issues in China.
720 *The Lancet* **381**, 2044–2053 (2013).
- 721 18. He, P., Baiocchi, G., Hubacek, K., Feng, K. & Yu, Y. The environmental impacts of rapidly changing
722 diets and their nutritional quality in China. *Nature Sustainability* **1**, 122–127 (2018).
- 723 19. Adalibieke, W. et al. Decoupling between ammonia emission and crop production in China due to
724 policy interventions. *Global Change Biology* **27**, 5877–5888 (2021).
- 725 20. Wang, C. et al. A high-resolution ammonia emission inventory for cropland and livestock production
726 in China. *Chinese Journal of Eco-Agriculture* **29**, 1973–1980 (2021).
- 727 21. Meng, W. et al. Improvement of a global high-resolution ammonia emission inventory for
728 combustion and industrial sources with new data from the residential and transportation sectors.
729 *Environmental science & technology* **51**, 2821–2829 (2017).
- 730 22. Huang, Y. et al. Quantification of global primary emissions of PM_{2.5}, PM₁₀, and TSP from combustion
731 and industrial process sources. *Environmental science & technology* **48**, 13834–13843 (2014).
- 732 23. Huang, T. et al. Spatial and temporal trends in global emissions of nitrogen oxides from 1960 to 2014.
733 *Environmental science & technology* **51**, 7992–8000 (2017).

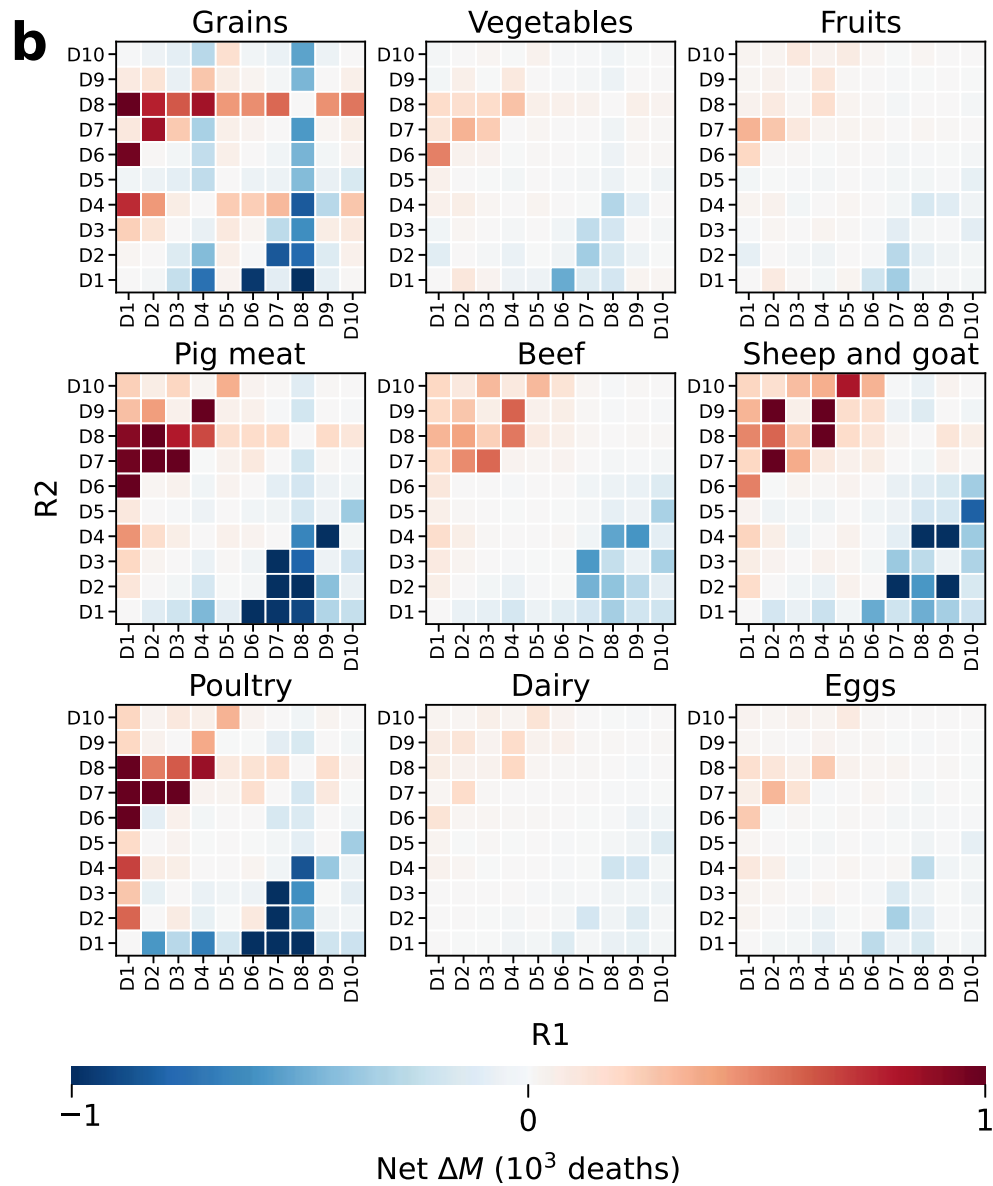
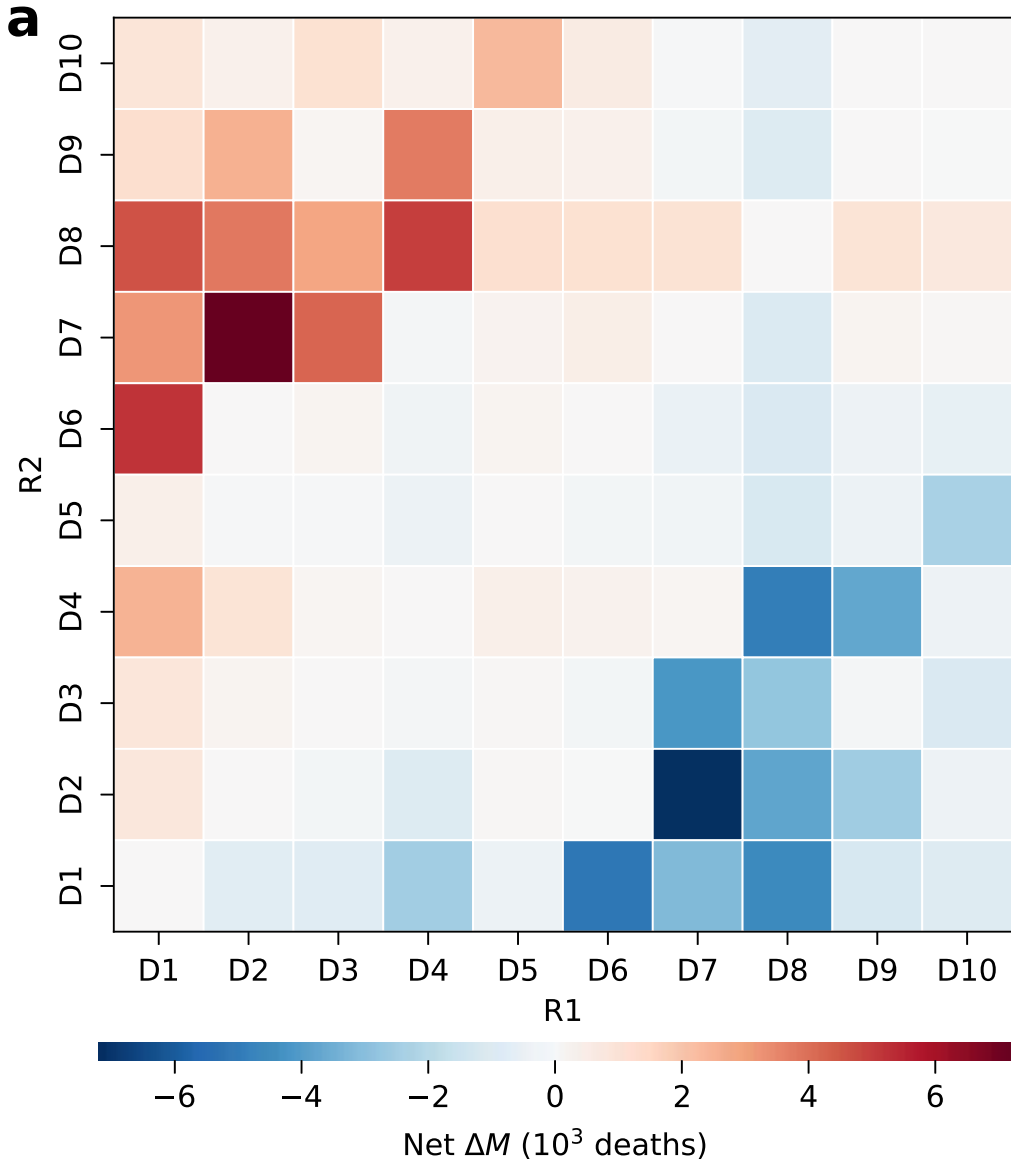
- 734 24. Huang, Y. *et al.* Global organic carbon emissions from primary sources from 1960 to 2009.
735 *Atmospheric Environment* **122**, 505-512 (2015).
- 736 25. Xu, H. *et al.* Updated global black carbon emissions from 1960 to 2017: improvements, trends, and
737 drivers. *Environmental Science & Technology* **55**, 7869-7879 (2021).
- 738 26. Zhao, S. *et al.* A multiphase CMAQ version 5.0 adjoint. *Geoscientific Model Development* **13**, 2925-
739 2944 (2020).
- 740 27. Sans, P. & Combris, P. World meat consumption patterns: An overview of the last fifty years (1961–
741 2011). *Meat Science* **109**, 106-111 (2015).
- 742 28. Bell, W., Lividini, K. & Masters, W. A. Global dietary convergence from 1970 to 2010 altered inequality
743 in agriculture, nutrition and health. *Nature Food* **2**, 156-165 (2021).
- 744 29. Ma, L., Long, H., Tu, S., Zhang, Y. & Zheng, Y. Farmland transition in China and its policy implications.
745 *Land Use Policy* **92**, 104470 (2020).
- 746 30. Xue, L. *et al.* China's food loss and waste embodies increasing environmental impacts. *Nature Food*
747 **2**, 519-528 (2021).
- 748 31. Maclean, W. *et al.* Food energy—methods of analysis and conversion factors. *Food and agriculture*
749 *organization of the united nations technical workshop report* (2003).
- 750 32. Kang, J. *et al.* Ammonia mitigation campaign with smallholder farmers improves air quality while
751 ensuring high cereal production. *Nature Food*, 1-11 (2023).
- 752 33. Institute for Health Metrics and Evaluation (IHME), *The Cost of Air Pollution: Strengthening the*
753 *Economic Case for Action*; 2016. <http://hdl.handle.net/10986/25013>.
- 754 34. *UN Sustainable Development Goals. Goal 10: Reduce inequality within and among countries.* (UN
755 Sustainable development group, 2022); <https://www.un.org/sustainabledevelopment/inequality/>
- 756 35. Zhai, F. *et al.* Prospective study on nutrition transition in China. *Nutrition reviews* **67**, S56-S61 (2009).
- 757 36. Xu, W. *et al.* Increasing importance of ammonia emission abatement in PM_{2.5} pollution control.
758 *Science Bulletin* (2022).
- 759 37. Chen, Y., Shen, H. & Russell, A. G. Current and future responses of aerosol pH and composition in
760 the US to declining SO₂ emissions and increasing NH₃ emissions. *Environmental Science &*
761 *Technology* **53**, 9646-9655 (2019).
- 762 38. Zheng, H. *et al.* Chinese provincial multi-regional input-output database for 2012, 2015, and 2017.
763 *Scientific Data* **8**, 244 (2021).
- 764 39. Burnett, R. *et al.* Global estimates of mortality associated with long-term exposure to outdoor fine
765 particulate matter. *Proceedings of the National Academy of Sciences* **115**, 9592-9597 (2018).
- 766 40. *FAOSTAT: FAO Statistical Databases.* <http://www.fao.org/faostat/en/> (Food and Agriculture
767 Organization of the United Nations, 2017).
- 768 41. Liu, X. *et al.* Dietary shifts can reduce premature deaths related to particulate matter pollution in
769 China. *Nature Food* **2**, 997-1004 (2021).
- 770 42. NBS. *China energy statistical yearbook 2017.* (China Statistics Press, 2017).
- 771 43. Zhao, H. *et al.* Assessment of China's virtual air pollution transport embodied in trade by using a
772 consumption-based emission inventory. *Atmospheric Chemistry and Physics* **15**, 5443-5456 (2015).
- 773 44. Shen, H. *et al.* Novel method for ozone isopleth construction and diagnosis for the ozone control
774 strategy of Chinese cities. *Environmental Science & Technology* **55**, 15625-15636 (2021).
- 775 45. Zhou, M. *et al.* Mortality, morbidity, and risk factors in China and its provinces, 1990–2017: a
776 systematic analysis for the Global Burden of Disease Study 2017. *The Lancet* **394**, 1145-1158 (2019).
- 777 46. Wang, X. *et al.* Sensitivities of ozone air pollution in the Beijing–Tianjin–Hebei area to local and

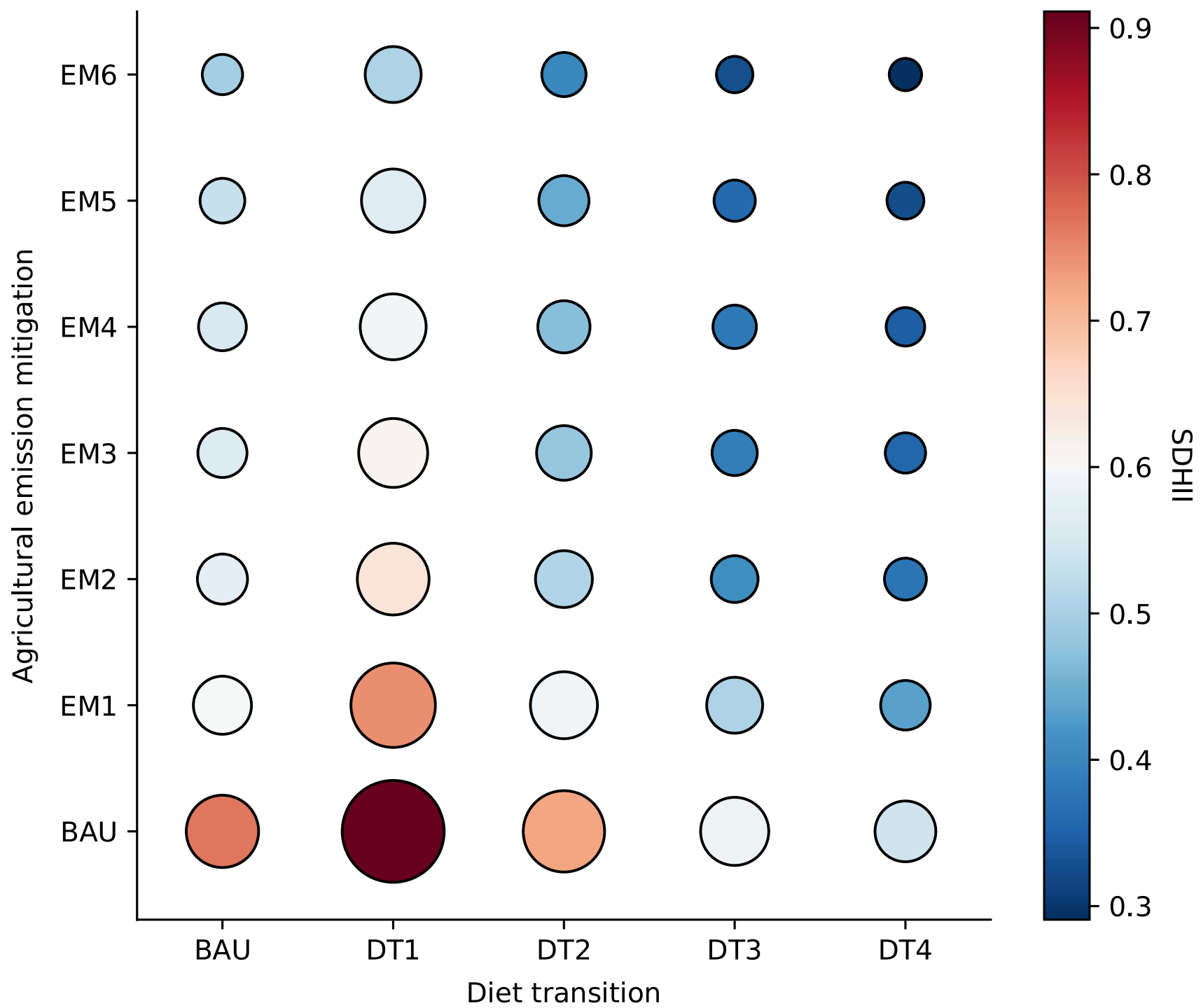
- 778 upwind precursor emissions using adjoint modeling. *Environmental Science & Technology* **55**, 5752-
779 5762 (2021).
- 780 47. Pappin, A. J. & Hakami, A. Source attribution of health benefits from air pollution abatement in
781 Canada and the United States: an adjoint sensitivity analysis. *Environmental Health Perspectives* **121**,
782 572-579 (2013).
- 783 48. Wang, M., Yim, S. H., Dong, G., Ho, K. & Wong, D. Mapping ozone source-receptor relationship and
784 apportioning the health impact in the Pearl River Delta region using adjoint sensitivity analysis.
785 *Atmospheric Environment* **222**, 117026 (2020).
- 786 49. Zhang, X. et al. Societal benefits of halving agricultural ammonia emissions in China far exceed the
787 abatement costs. *Nature Communications* **11**, 4357 (2020).
- 788 50. Zhang, C., Ju, X., Powlson, D., Oenema, O. & Smith, P. Nitrogen surplus benchmarks for controlling N
789 pollution in the main cropping systems of China. *Environmental Science & Technology* **53**, 6678-6687
790 (2019).
- 791 51. Panel, E. N. E. Nitrogen use efficiency (NUE): an indicator for the utilization of nitrogen in food
792 systems. *Wageningen University, Alterra, Wageningen, Netherlands* (2015).
- 793 52. Hong, C. et al. Global and regional drivers of land-use emissions in 1961–2017. *Nature* **589**, 554-561
794 (2021).











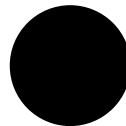
Mortalities



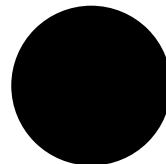
1×10^5



2×10^5



3×10^5



4×10^5